Wear 271 (2011) 364–373

Contents lists available at ScienceDirect

Wear

journal homepage: www.elsevier.com/locate/wear

Advanced metallurgical alloy design and thermomechanical processing for rails steels for North American heavy haul use

R. Ordóñez Olivares[a], C.I. Garcia[a], A. DeArdo[a], S. Kalay[b], F.C. Robles Hernández[b,c,*,1]

[a] University of Pittsburg, Mechanical and Materials Science and Engineering Department, 648 Benedum Hall, 3700 O'Hara Street, Pittsburgh, PA 15261, USA
[b] Transportation Technology Center, Inc., 55500 DOT Road, Pueblo, CO 81001, USA
[c] University of Houston, College of Technology, 304A Technology Building, Houston, TX 77204-4020, USA

ARTICLE INFO

Article history:
Received 24 September 2010
Accepted 3 October 2010
Available online 20 October 2010

Keywords:
Premium rail steel
Advanced rail steel
Microstructure
Characterization
Thermo-mechanical processing (TMP)
Rolling contact fatigue (RCF)

ABSTRACT

Rail is the most valuable asset owned by railroads the AAR reported that only in North America the annual expenditure for rail repair and replacement is approximately $2.6 billion. In the last 50 years the railways and rail manufacturers have improved rail performance. Modern rail metallurgies have achieved a successful increased in hardness from 248 Hardness Brinell (HB) to more than 400 HB. This in turn increased the wear resistance of rails and a life extension. Lubrication and suspension bogies have positively contributed to rail life extension as well. Unfortunately, not as much progress has been made as far as rail's fatigue performance (e.g. rolling contact fatigue (RCF)), and fracture toughness. In this work is presented a methodology followed to development a new metallurgy that will increase RCF and wear resistance. The development of this new rail consists of rail characterization and advanced rail steel design.

Published by Elsevier B.V.

1. Introduction

Clayton et al. made one of the most extensive research works of rail's wear and rail's life extension for various metallurgies for several years [1–7]. Clayton et al. contemplated in his publications the effects of heat treatment [1], interlamellar spacing [2], microstructure [3,5], track curvature [6] among other rail and track characteristics. In the last 50 years the railways and rail manufacturers had improved rail performance by increasing hardness from 248 HB to more than 400 HB. The use of premium rail in North America is mainly in use along curves and inclined tracks; although, some railroads started using premium rails in tangent tracks where the yearly transit exceeds 40,000–60,000 MGT. Fig. 1 illustrates the historical path followed in the development of the current premium rail steel metallurgies. Although current rail steels used in North America have good wear resistance, RCF improvements are necessary since a great portion of the rails are removed prematurely mainly due to fatigue related issues. It is important to mention that the RCF also depends on the loading environment, impact characteristics, creepage and other contact related phenomena. Therefore, rails used in heavy haul lines in North America may experience more RCF than the same rail in railroad lines with more moderate loading environment.

Beynon et al. [8] showed that nonmetallic inclusions have direct effects on RCF development. A major finding in the railroad industry is the determination of the effects of cleanliness on railroad track components subjected to contact fatigue (rail, wheels, bearings, etc.) [9–12]. In order to meet the future requirements of heavy haul railroads in the USA, the Transportation Technology Center, Inc. (TTCI) conducted a major effort to develop a new rail steel that possesses superior wear resistance properties and significantly higher RCF and wear resistance. Under the scope of this rail steel development it has been determined that hyper-eutectoid steels with pearlitic microstructure may be the most suitable steels to guarantee rail's life extension [9]. TTCI and the University of Pittsburgh found that pro-eutectoid cementite along the prior austenite grain boundaries is the main factor that may have negative effects on fracture toughness, elongation, fatigue, and wear resistance on hypereutectoid pearlitic rail steels [12–14]. It is important to mention that not all premium rails show pro-eutectoid cementite and the amount vary for the different manufacturers.

This project had been divided in two sections; in Phase I was conducted a thorough metallurgical analysis and characterization of the microstructures of two generation of premium rail steels (13 different types of rails in total). The investigated rails were

* Corresponding author. Current address: University of Houston, College of Technology, 304A Technology Building, Houston, TX 77204-4020, USA.
Tel.: +1 713 743 8231; fax: +1 505 213 7106.
E-mail address: fcrobles@uh.edu (F.C. Robles Hernández).
[1] Formerly at TTCI and currently at the Mechanical Engineering Technology Department at the University of Houston.

0043-1648/$ – see front matter. Published by Elsevier B.V.
doi:10.1016/j.wear.2010.10.048

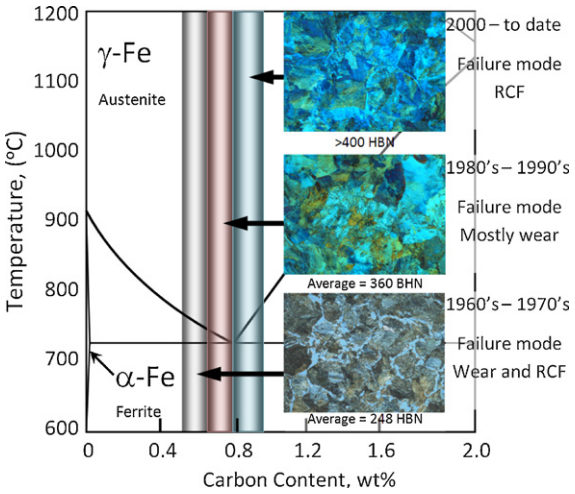

Fig. 1. 50 years evolution of rail steel metallurgies for heavy haul use in North America.

manufactured in 2001 and 2005 by Corus, JFE Steel America Inc., Mittal, Nippon Steel Corporation, Rocky Mountains Steel Mills, and Voestalpine. Phase I has been accomplished using optical and scanning electron microscopy (SEM) techniques to determine microstructural characteristics such as: interlamellar spacing, pearlite colony size, and prior austenite grains. This helped to complete knowledge of the effects that microstructural constituents on mechanical properties and field service characteristics of rail steels. Rails in new and service conditions were investigated.

In Phase II is used the knowledge gained in Phase I to conduct an advanced design of the next generation premium rail steel with higher wear and fatigue resistance. As of today, rail steel metallurgies are reaching a limit of development; although, thermomechanical processing (TMP) is believed to be able to further increase yield strength (YS) or proof stress for typical premium rail chemistries. In addition, advanced alloy design will further increase the potential to maximize rail performance. The idea in this Phase is to design a functional alloy capable of having a narrower interlamellar spacing that is susceptible to further refinement during thermomechanical processing with low level of inclusions. The implementation of the TMP will yield homogenous microstructures and may increase the rail's hardness and hence significant improvements in rail RCF performance.

In this paper are described the laboratory test results and the procedures followed to develop this advance steel as well as the steps followed to designed the optimum TMP to achieve the desired microstructure. Following the completion of the laboratory testing, the best performing steel and TMP were used to cast and roll a heat of rail steel. In the present work are proposed 5 steels and one of which was selected as a candidate to cast a heat of steel and roll rails with this specific composition. The rail with best mechanical properties and most promising is characteristics is identified in this paper as RS2 was cast and rolled by Voestalpine, such rail is currently in process of installation at the Facility for Accelerated Service Testing (FAST) at TTCI, Pueblo, Colorado (fall 2010). The rail will be tested along with rails from other manufacturers to have a direct rail performance comparison.

2. Phase I – analysis of nonmetallic inclusions

Modern higher strength rail steels have a tighter control of nonmetallic inclusions, primarily oxides and sulfides. In the investigated rails has been found by SEM that the volume fraction of nonmetallic inclusions is comparable in all rails. However, the cleanliness results conducted by optical means based on the E45 and E1245 ASTM standards [15,16] indicate that the cleanliness levels of each steel are different particularly the number, type, and shape. The cleanliness results obtained from the E45 and E1245 ASTM standards can be consulted in Ref. [10]. These observations imply that the rail manufacturers may use different technologies to produce the premium rail steels. Additionally, the investigated rails presented different amounts of pro-eutectoid cementite. Revealing pro-eutectoid cementite by chemical means is challenging and the results of this phase presented in this work were simulated using the JMatPro4.0 software. The metallographic determination of the amount of pro-eutectoid cementite is contemplated for future publications.

The majority of the observed inclusions were MnS and Al_2O_3, and some of the investigated steels contained complex oxide inclusions. Fig. 2 shows some examples of the typical inclusions and pro-eutectoid cementite present in the investigated rail steels. Preliminary analysis of the inclusions indicates that their numbers and fraction volume (including voids) may have secondary effects on fatigue performance. In contrast, parameters such as particle size, type, distribution, and shape are more detrimental and can contribute to excessive RCF and the premature removal of the rail [10]. In Table 1 are presented the results of SEM analysis for the investigated (commercial) premium rails, the highlighted steels correspond to the cleanest and dirtiest microstructures as per SEM analysis.

Nonmetallic inclusions can have a negative effect on the nucleation and propagation of defects (including RCF cracks), but it seems that for premium rail steels, the presence of pro-eutectoid cementite has a direct influence/effect on RCF formation. Potentially, the major finding of this work is the effect of pro-eutectoid cementite on RCF. Fig. 3 shows some of the microstructural analysis conducted on the investigated rail steels. These micrographs indicate typical interlamellar pearlitic structure and a transgranular crack behavior in samples exhibiting RCF. Analysis shows that the cracks growth along the grain boundaries in a trans-granular fashion along the prior-austenite grain boundaries. The pro-eutectoid cementite is mainly identified along the grain boundaries that are relatively weaker locations where the cracks are initiated. Fig. 3 indicates a series of micrographs with transgranular cracking along the prior-austenite grain boundaries with some pro-eutectoid cementite. The limited amount of pro-eutectoid cementite present in these micrographs is attributed to a potential removal during polishing and etching. The secondary cracking is usually influenced by the presence of hard inclusions (e.g. Al_2O_3, complex oxides). Therefore, in order to minimize RCF, pro-eutectoid cementite and hard inclusions, should be minimized and ideally eliminated.

The preliminary results of this study showed that the major metallurgical factors contributing to the strength of fully pearlitic steels are (a) solid solution strengthening, (b) pearlite colony size, (c) interlamellar spacing, and to a lesser extent (d) the austenite grain size. The transformation behavior of the austenite also controls the presence of pro-eutectoid cementite, which should be minimized or eliminated. It is suggested that a pearlitic microstructure with a fine interlamellar spacing and thinner cementite lamellae could improve wear and RCF performance. This and other approaches have been explored in this research work to improve not only wear, but also RCF performance for this new rail steel metallurgy by reducing the amounts of pro-eutectoid cementite and inclusions. Table 2 summarizes the influence of microstructural defects on mechanical characteristics on commercial rail steels. This table indicates the main microstructural factors responsible for the in-service performance of rail steels.

Fig. 4 sketches the procedure followed in Phase I to determine the main microstructural characteristics. Table 3 presents a summary of all the microstructural characteristics for all the rails

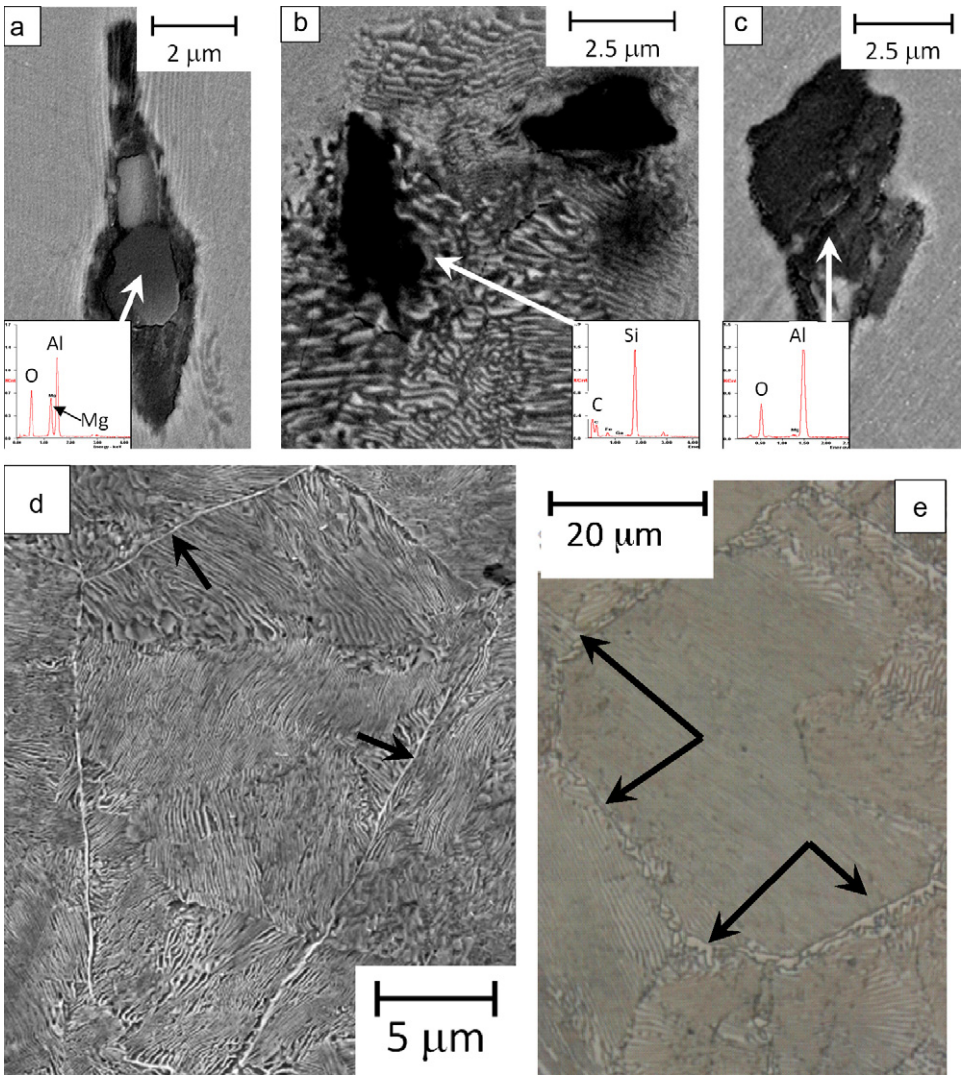

Fig. 2. Typical inclusions identified in the investigated rail steels: (a) mixed of oxide inclusions of alumina (Al_2O_3) and magnesium oxide (MgO), (b) silicon carbide (SiC), (c) Al_2O_3 inclusions, and (c, d) pro-eutectoid cementite along the prior-austenite grain boundaries by means of SEM and optical microscopy respectively.

Table 1
Results of the inclusion content and identification measured by SEM/EDS on the investigated premium rails. Highlighted text (rails J and D) are indicating the rails with the lowest and largest amounts of inclusions respectively.

Generation	ID	$Vf_{Sulfides}$	Vf_{Oxides}	Vf_{Total}	Types
2000	A	0.005272	0.000824	0.006096	MnS, SiC
	B	0.000928	0.00058	0.00151	Al_2O_3, MnS
	J	0.00022	0.000682	*0.00091*	Al_2O_3, MnS
	K	0.0131	0.003159	*0.01621*	
	M	0.00097	0.000201	0.00117	
	L	0.00109	0.000255	0.00134	Al_2O_3, MnS, $CaCO_3$, $MgCO_3$, TiN
2005	C	0.00304	0.00216	0.00519	Al_2O_3, MnS
	D	0.01655	0.007839	*0.02439*	Al_2O_3, MnS, SiC
	E	0.00112	0.000191	0.00131	MnS, SiC
	F	0.000861	0.000546	0.00141	Al_2O_3, MnS, $CaCO_3$, $MgCO_3$
	G	0.00088	0.000299	0.00118	TiN, Al_2O_3, MnS, SiC
	I	0.00087	0.000332	0.00120	TiN, VN, SiC, Al_2O_3

Table 2
Microstructural factors that have a direct contribution to rail performance. Relative influences: + medium influence, ++ high influence, – no influence.

	Pro-eutectoid cementite	Non metallic inclusions	Austenite grain size	Interlamellar spacing
Rolling contact fatigue	++	++	++	++
Impact toughness	++	+	++	++
Wear	+	+	–	+

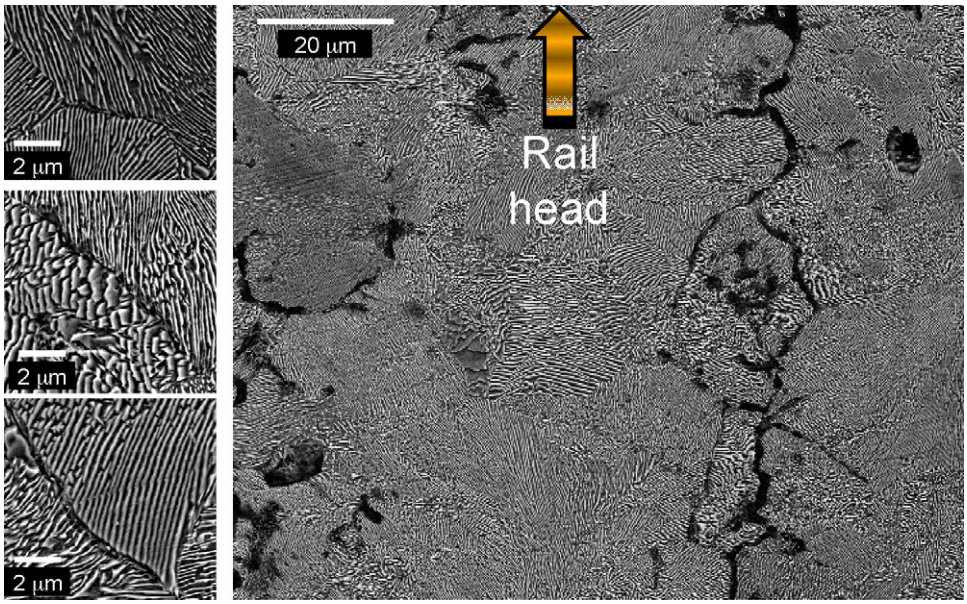

Fig. 3. Scanning electron micrographs indicating intergranular cracking (RCF) along the prior-austenite grain boundaries in the presence of pro-eutectoid cementite. Note: some of the pro-eutectoid cementite may be lost due to its lack of integrity (following the cracking), sample handling, polishing and etching resulting in the limited amount of this phase observed in the above micrographs.

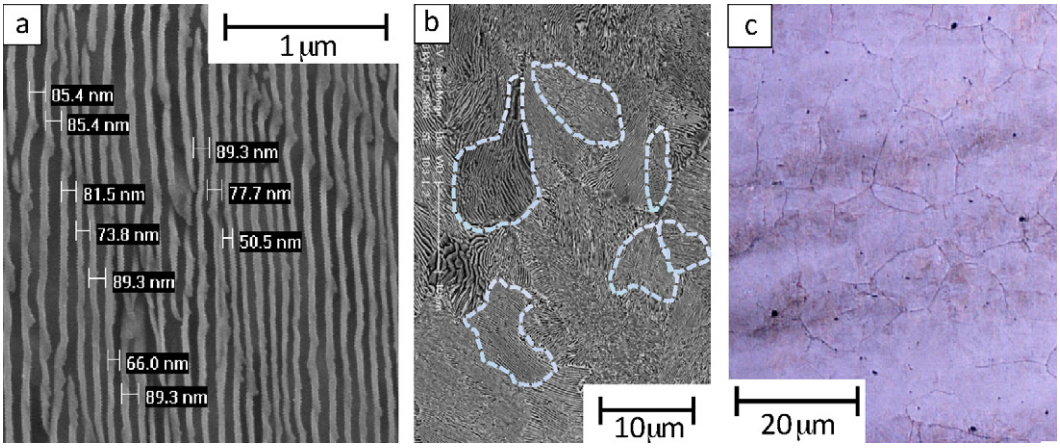

Fig. 4. Brief summary of the microstructural analysis for (a) interlamellar spacing, (b) pearlite colony size, and (c) prior-austenite grain conducted on premium rails (Phase I).

Table 3
Summary of results of microstructural characterization conducted on the rails investigated in Phase I. IS, PCS, and PAGS stand for interlamellar spacing, pearlite colony size and prior-austenite grain size respectively.

Year	ID	Head			Web			Base		
		IS	PCS	PAGS	IS	PCS	PAGS	IS	PCS	PAGS
2000	A	0.10	2.6	67.9	0.15	3.3	74.4	0.15	3.2	21.3
	B	0.10	1.9	59.4	0.13	3.5	32.1	0.13	2.4	27.3
	J	0.08	2.4	32.4	0.13	2.5	60.86	0.18	4.4	27.3
	K	0.08	2.5	64.3	0.18	4.1	73.1	0.15	3.8	28.3
	M	0.10	3.0	56.25	0.13	3.9	66.3	0.15	3.3	23.1
	L	0.10	2.9	49.8	0.13	2.9	34.28	0.15	3.5	23.2
2005	C	0.09	2.1	34.7	0.15	3.5	64.6	0.20	4.2	21.0
	D	0.09	2.0	34.7	0.15	4.5	27.2	0.19	3.9	28.5
	E	0.09	2.8	28.8	0.15	3.9	32.1	0.16	3.6	26.3
	F	0.12	2.8	23.3	0.12	3.6	32.0	0.12	3.1	22.1
	G	0.07	2.8	24.8	0.11	4.3	27.88	0.13	3.2	22.2
	H	0.10	2.9	25.9	0.13	3.8	47.8	0.15	2.9	23.9
	1	0.09	2.7	58.6	0.15	2.7	61.48	0.18	3.9	20.51

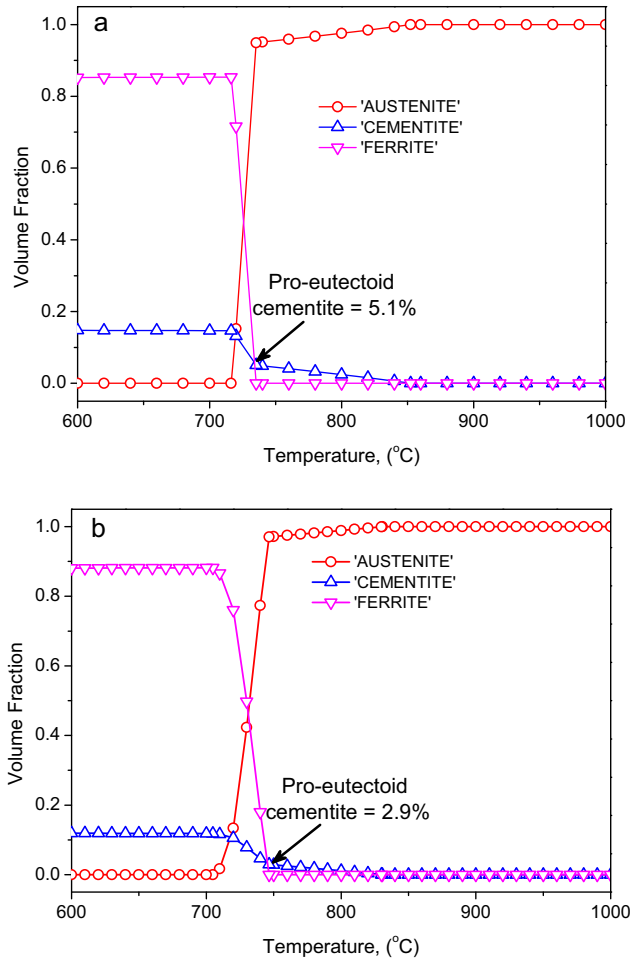

Fig. 5. JMatPro4.0 simulations for (a) commercial steel (ID as M) and (b) the experimental steel R2. The design process of steel R2 is explained in detail in Phase II.

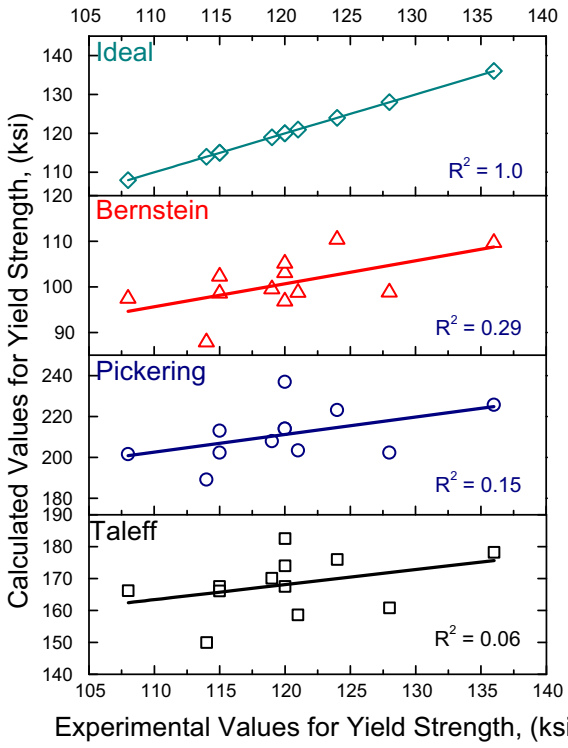

Fig. 6. Numerical models correlating calculated and experimental values of yield strength.

manufactured in 2001 and 2005. Two hundred measurements per location (head, web and base) for interlamellar spacing, the pearlite colony size and prior-austenite grain size were carried out in per rail steel. From Table 3 can be observed that in average the interlamellar spacing along the head of the rail is in most cases the smallest when compared to the measured values from the rails web and base and the same trend is observed for the pearlite colony size. The prior-austenite grain size the values in the head are smaller than the web, but the smallest values are identified along the base of the rail.

Pro-eutectoid cementite is the most detrimental microstructural feature for RCF performance. However, its precise quantification by conventional metallographic methods is challenging and represents an outstanding effort. In contrast the amount of pro-eutectoid cementite for each of the compositions can be estimated by numerical simulations using JMatPro4.0. As examples of the JMatPro4.0 simulations Fig. 5 shows a commercial premium rail steel (M) composition and one the experimental steel identified as (RS2) developed in Phase II of this work. The simulations shown in Fig. 5 were conducted based on the chemical composition of each steel and its grain size as determined experimentally (Table 3).

The volume fraction of pro-eutectoid cementite is as the amount of cementite that precipitates at the eutectoid temperature. Any temperature below the eutectoid promotes the precipitation of pearlite and hinders any further precipitation of pro-eutectoid cementite. In Fig. 5 the eutectoid temperature can be better distinguish as the intersection among ferrite and cementite lines. In other words, the amount of cementite that precipitates above the eutectoid temperature is the pro-eutectoid cementite that is be observed along the grain boundaries (Figs. 2 and 3). From Fig. 5 can be mentioned that the experimental steel Rs2 has a significantly lower amount of pro-eutectoid cementite than the commercial M steel and this can be translated into a better RCF resistance.

In the literature are found empirical approximations that correlate steel microstructural characteristics to mechanical properties. In the literature were identified three numerical models as approximations. This is of great interest because by proposing a specific composition it is possible to use software such as JMatPro4.0 and determine the exact cooling conditions (continuous cooling transformation (CCT) diagrams) to obtain specific microstructural characteristics. This information is used to extrapolate mechanical properties by using the methods reported in the literature (Fig. 6) [19–21]. The "ideal" case in Fig. 6 was developed using the results from Phase I and is capable of predicting the yield strength of hypereutectoid steels as a function of its microstructural characteristics. This is of great interest because by using software such as JMatPro4.0 it is possible to assess the required cooling path in order to achieve a specific microstructure hence the desired mechanical properties.

Fig. 6 shows a series of graphs with the calculated vs analytical results of the yield strength for the investigated premium rails steels using the three different approximations found in the literature [19–21]. These methods show a weak correlation with the experimental values and either underestimates or overestimates the values for yield strength. In addition to that the R^2 is too low, which further confirms the weakness of these approximations. Therefore, a more sophisticated model has been developed by researchers from University of Pittsburgh and such model approaches more closely the curved identified as "ideal" condition. Similar approach was published by Clayton et al. [2] shows an exponential behavior among interlamellar spacing (100–500 nm) and hardness. In Fig. 7 similar procedure is followed and the relation

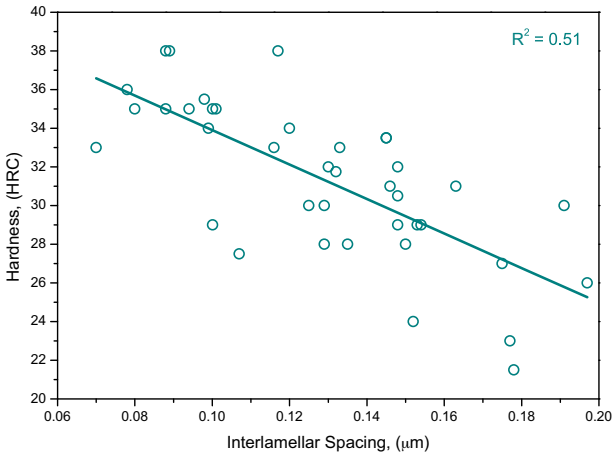

Fig. 7. Relationship among pearlite interlamellar spacing and Rockwell C hardness.

that better satisfied the interlamellar spacing to hardness is quasi-linear (Fig. 7) that is attributed to the narrow range of interlamellar spacings in the investigated for premium rail steels (70–197 nm).

The steels proposed in Phase II were designed based on the algorithms developed by the University of Pittsburgh for hardness and yield strength determination. The above-mentioned algorithms are considered for future publications. The final microstructure of the rails metallurgies proposed in Phase II were first design by means of numerical simulations using the JMatPro4.0 software before the short heats were cast. Once the microstructure is design the determination of the mechanical properties is conducted by means of the algorithms developed by the University of Pittsburgh. From Figs. 6 and 7 shows the better fit of the ideal approximation that was used as a based model for the determination of the optimum properties for rail steels a function of the microstructural characteristics.

3. Phase II – Research and Development (R&D) Program

The R&D of the next generation of rail steel is summarized in the flowchart in Fig. 8, which indicates the process followed to address the most important aspects of advanced steel design and development. A schematic of the TMP conducted for the experimental rail steels is also shown. Five premium rail steels were design in this project. Four of the rail compositions were pearlitic and one was bainitic. Carbon content ranged from 0.7 wt%C to 0.85 wt%C for the pearlitic steels and 0.3 wt%C for the bainitic steel. Other alloy elements added to the proposed rail compositions included vanadium, molybdenum, niobium, manganese, and silicon. A tight control in the levels of phosphorus and sulfur was also implemented. The chemical compositions of the respective steels are currently confidential [24] the C, Mn, S and P contents are given in Table 4. Silicon increases the activity of carbon in both austenite and ferrite, thus reducing the local carbon activity gradient by slowing down the formation and growth of cementite [12,17]. Manganese has a small effect on the growth kinetics of cementite by reducing proeutectoid ferrite and increasing hardness. Manganese distributes preferentially to cementite and lowers the temperature at which

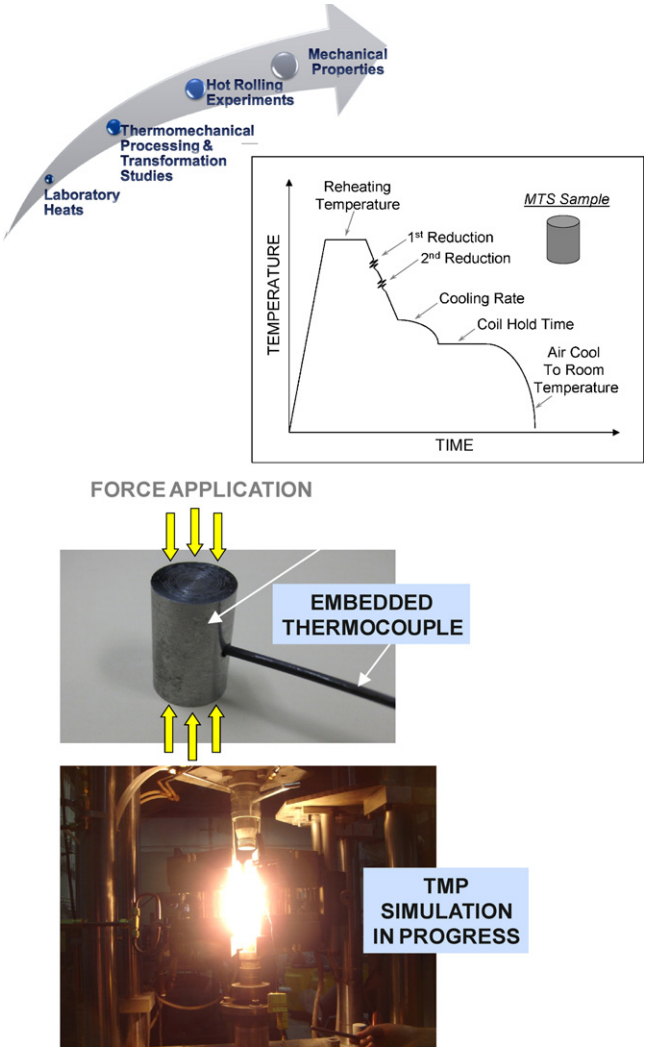

Fig. 8. Experimental procedure, and a schematic of the TMP and set up used during the design and development of the next generation of rail steels.

cementite begins to form. Chromium and silicon act in a synergistic manner improving the strength by solid solution strengthening and preventing the coarsening of cementite particles. Molybdenum has several effects on steels and for the purpose of this steel development. Molybdenum was selected for its positive effects on: carbide formation, hardenability, mechanical properties, pearlite stabilizer, and reduce embrittlement. Niobium was added to the experimental steel compositions due to its effects on austenite grain size, and grain size control. Vanadium has positive effects in pearlitic steels due to its effects on hardening, austenite grain size, mechanical properties, and grain size control [25].

Fig. 9 presents the theoretical continuous cooling transformation (CCT) diagrams of the laboratory heats. The CCT diagrams for different rail steels cooled at variable rates were numerically determined by utilizing the thermodynamic model JMatPro4.0. The CCT diagrams show that the same steel composition can produce a

Table 4
Partial chemical compositions of the experimental steels the other elements (Ni, Cr, Mo, V, Al, Cu, Nb, and N) are confidential [25].

Elements	Rsteel 1	Rsteel 2	Rsteel 3	Rsteel 4	Rsteel 5
C	0.70–0.80	0.75–0.85	0.80–0.90	0.28–0.32	0.85–0.90
Mn	1.00–1.10	1.10–1.20	1.00–1.10	1.90–1.20	1.10–1.25
P	0.005–0.007	0.005–0.007	0.005–0.007	0.005_{max}	0.005_{max}
S	0.003_{max}	0.003_{max}	0.003_{max}	0.003_{max}	0.003_{max}

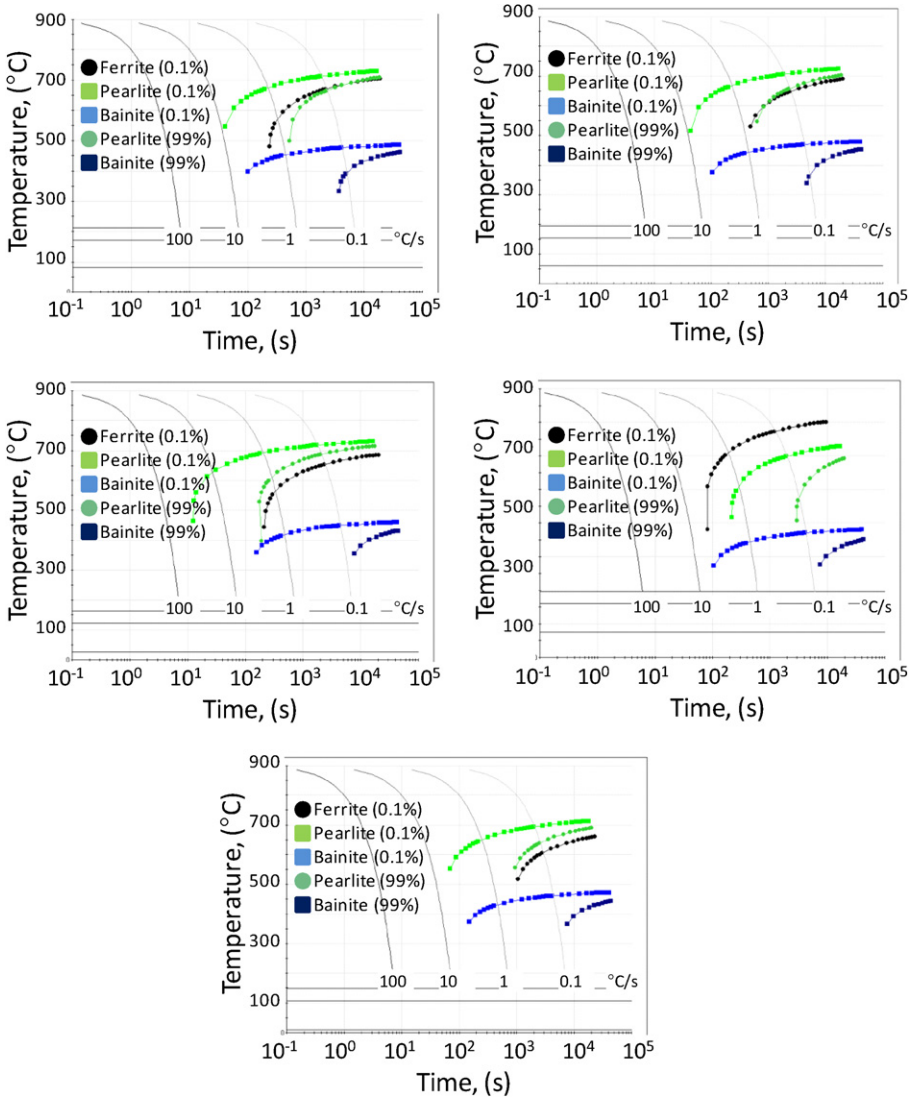

Fig. 9. Continuous cooling transformation (CCT) curves of the experimental steels designed in Phase II.

large range of microstructural conditions from fully pearlitic, to bainitic to martensitic microstructures, or combinations thereof, which are achieved at different cooling rates. Therefore, controlling the cooling rate is important and this will determine the final microstructure in the rails. In addition, alloy designs open the potential for further optimization for rail steels. The JMatPro4.0 software was used to determine the microstructural state of the austenite prior to transformation and the determination of the pro-eutectoid cementite expected for a specific thermal path.

Fig. 10 shows the results of the predicted amounts of pro-eutectoid cementite in the commercial and the experimental rail steels. It is important to mention that the amount of pro-eutectoid cementite in the experimental steels is lower than in most commercial rail steels. This is attributed to the lower carbon contents in the experimental steels. The reduced amount of pro-eutectoid cementite that may form along the prior-austenite grains in this newly developed rail steels is expected to retard the development of RCF in rails subjected to North American heavy haul environments. Table 4 shows partial chemical compositions of the R1–R5 experimental steels.

By comparing the amounts of pro-eutectoid cementite in commercial and experimental rails (Fig. 10) can be observed that some of the commercial rail steels have comparable amounts of pro-eutectoid cementite to the rails proposed in the present research. For instance, in a rail performance test conducted at FAST, Rail K did not need grinding after 478 MGT of heavy haul traffic, which means the amount of RCF was low to moderate under non-lubricated conditions. On the other hand, Rail L exhibited severe RCF and required grinding after 270 MGT [9,11]. Therefore, due to the amount of pro-

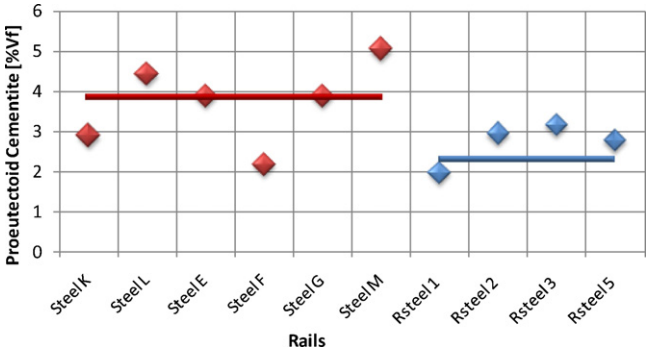

Fig. 10. Comparison of the JAtPro4.0 calculated volume fraction (Vf) of pro-eutectoid cementite in the commercial rail steels, and in the laboratory heats.

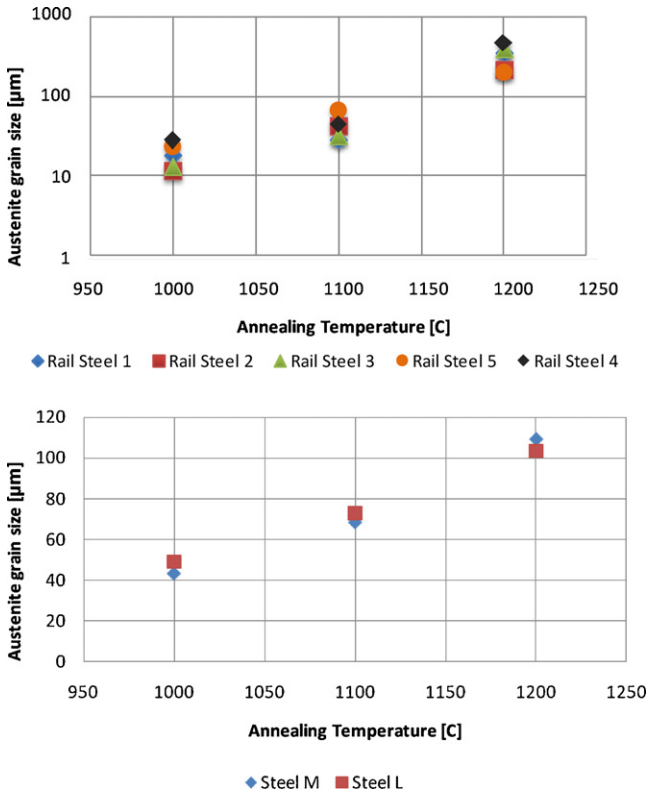

Fig. 11. Austenite grain growth of selected commercial rail steels, and the 5 experimental steels developed under the scope of this project.

eutectoid cementite in the experimental rails it is expected that they may have similar or better RCF resistance than rail K (Fig. 10). These results indicate that a lower amount of pro-eutectoid cementite may retard RCF, which leads us to conclude that designing rail steels with lower amounts of pro-eutectoid cementite in the experimental steels can reduce RCF.

4. TMP of commercial and laboratory steels

Prior to any deformation studies, the grain coarsening behavior of selected commercially available rail steels and all the experimental steels were studied. Fig. 11 shows an example of the austenite grain coarsening behavior for steels M and L, as well as the experimental steels (1–5) to show the coarsening kinetics of the rail steels. The grain coarsening ability in the experimental steels is quite diverse when compared to the commercial steels. This difference is attributed to the superior cleanliness of the experimental steels. The coarsening effect in commercial premium rail steels is limited by the presence of inclusions that are acting as barriers to grain growth, and behave as grain stabilizers instead.

As per the Hall–Petch relationship [22,23] grain refinements is of great importance, and in this work the TMP is designed to refine the grain as effectively as possible. The optimization of the TMP enhances static and dynamic recrystallization allowing the refinement of the experimental steel microstructures. It is expected that this will maximize the rail performance characteristics. In order to accomplish the desire microstructure, it is important to understand the microstructural state of the austenite prior to any hot deformation or transformation. Using Fig. 11 can be determined the optimum annealing temperature to start the TMP.

The state of austenite prior to transformation has a significant impact on the morphology of the pearlite, and the formation of pro-eutectoid cementite by controlling the transformation temperatures. Fig. 11 shows the effect of annealing temperature on grain sizes. During annealing the grain size is optimized and then is refined dynamically and statically during the TMP. Further, the superior cleanliness of in the RS1-RS5 allows a complete control of the grain size, which may not be possible with the commercial rail steels. In addition, the effect of cooling rate, as shown in Fig. 9 it has to be tightly monitored. In the experimental trials all the above results were taken under consideration to control the decomposition behavior of the microstructure, and the formation of pro-eutectoid cementite along the prior austenite grain boundaries.

A short heat per composition was cast under vacuum conditions to obtain ingots of 100–150 lbs per composition. The short heat ingots were hot processed to obtain plates of approximately 1 in thickness. Fig. 12 presents pictures of the ingot as well as the hot plates. The plates seen in Fig. 12 were hot rolled for the laboratory trials to understand the evolution of the microstructure for each composition and develop relationships among microstructure and mechanical properties. Fig. 12c shows the fashion in which the samples for the TMP (Fig. 8) simulations were extracted.

The corresponding strengthening mechanisms responsible for the development of the mechanical properties during TMP are currently under evaluation. This study will help in understanding the actual TMP conditions that will be targeted for steel mills. It is the

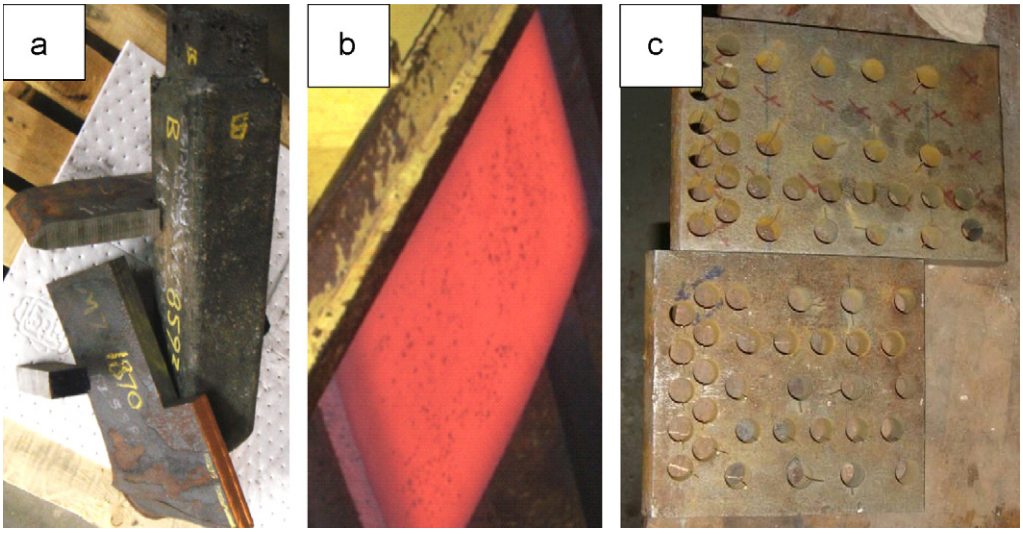

Fig. 12. (a) As cast ingot and hot-rolled plate at room temperature, (b) plate during hot rolling operation, (c) plate after the samples for TMP (Fig. 8) were removed.

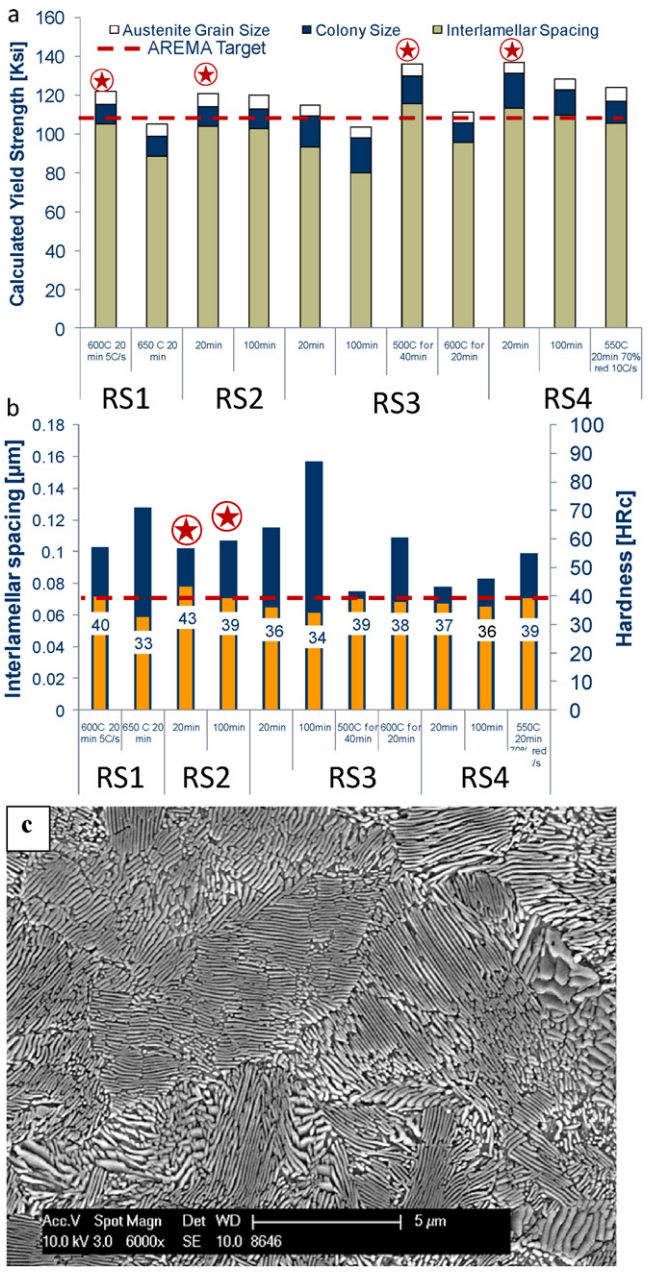

Fig. 13. (a) Calculated values of yield strength for a selected experimental steels, (b) hardness and interlamellar spacing of the various experimental steels (RS stands for rail steel), and (c) fully pearlitic microstructure.

intention of this work that similar procedures will be followed for commercial rail steels to optimize their microstructures in order to optimize their TMP. Following the TMP the microstructures are analyzed and the hardness was evaluated.

Fig. 13a shows the contribution of each of the microstructural characteristics of the as rolled steels on yield strength as determined by the numerical model developed by the University of Pittsburgh. Based on this prediction the steels microstructures with the best mechanical properties and a fully pearlitic microstructure were selected for hot rolling. Once the TMP is optimized the plates are heat treated and rolled under the exact temperature and deformation conditions to heat treat the plated for tensile, fracture toughness, wear, and hardness analysis using ASTM standards methods.

The microstructural conditions prior to transformation and cooling rate effects were used to evaluate the resulting pearlite

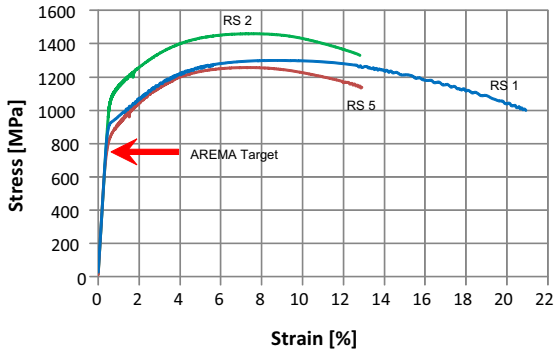

Fig. 14. Results of mechanical testing of experimental steels after rolling.

colony size and the interlamellar spacing, which is in agreement with Ref. [18]. The results of the TMP and cooling experiments were supported by a systematic dilatometric study of the decomposition of austenite. From the dilatometry results systematic microstructural and hardness evaluations were conducted. The steels that exhibited the best combination of fully homogenized microstructure and best mechanical properties (as predicted numerically using the "Ideal" model Fig. 6) for a given chemistry and TMP are indicated with an (★) in Fig. 13a. The steels and heat treatment conditions indicated with "★" were selected for the rolling process and the results are presented in Fig. 13b. The steels in the as rolled conditions are presented in Fig. 13b, rail RS2 is indicated with an ★ due to its superior characteristics its respective microstructure is given in Fig. 13c. In the laboratory conditions it was possible to heat treat RS2 and obtain a fully pearlitic microstructure. Tensile test results of selected experimental steels in as rolling conditions are presented in Fig. 14, the mechanical properties in the as TMP conditions are considerably higher. The results presented in Figs. 13b, c and 14 were used to selected the experimental RS2 as ideal candidate to manufacture the rail by Voestalpine.

5. Conclusions

Some premium rail steels exhibit pro-eutectoid cementite at the prior austenite grain boundaries. This phase has been identified as the major contributor to the development of RCF in the railhead. The presence of inclusions has been found to aggravate the problem, because they aid the development of secondary cracks in the rail. A number of other factors that affect impact toughness and wear have been identified as well. Advanced alloy design and TMP methods allowed the development of rail steel with limited to non pro-eutectoid cementite and ultra low levels of inclusions. The level of inclusions was achieved through a tight control of the rail chemistry (S and P) and vacuum degassing. The use of advanced TMP allowed the optimization of a fully pearlitic steel microstructure.

References

[1] V. Dikshit, P. Clayton, D. Christense, Investigation of rolling contact fatigue in a head-hardened rail, Wear 144 (1991) 89–102.
[2] P. Clayton, D. Danks, Effect of interlamellar spacing on the wear resistance of eutectoid steels under rolling-sliding conditions, Wear 135 (1990) 369–389.
[3] R. Devanathan, P. Clayton, Rolling-sliding wear behavior of three bainitic steels, Wear 151 (1991) 255–267.
[4] N. Jin, P. Clayton, Effect of microstructure on rolling/sliding wear of low carbon bainitic steels, Wear 202 (1997) 202–207.
[5] D. Danks, P. Clayton, Comparison of the wear process for Eutectoid rail steels and laboratory test, Wear 120 (1987) 233–250.
[6] P. Clayton, Predicting the wear of rails on curves from laboratory data, Wear 181–183 (1995) 11–19.
[7] P. Clayton, Tribological aspects of wheel-rail contact: a review of recent experimental research, Wear 191 (1996) 177–183.
[8] J.H. Beynon, J.E. Garnham, K.J. Sawley, Rolling contact fatigue of three pearlitic rail steels, Wear 192 (1996) 94–111.

[9] F.C. Robles Hernández, N.G. Demas, D.D. Davis, A.A. Polycarpou, L. Maal, Mechanical properties and wear performance, Wear 263 (2007) 766–772.
[10] F.C. Robles Hernández, J. LoPresti, Linking Fatigue, Microcleanliness, Tensile, and Fracture Toughness Tests, Technology Digest, TD-09-010, Association of American Railroads, Transportation Technology Center, Inc., 2009.
[11] F.C. Robles Hernández, et al., Tribo-characterization of premium rails and correlation between ball-on-disk and full-scale tests, Wear (2009), Submitted.
[12] F.C. Robles Hernandez, Semih Kalay, R. Ordoñez Olivares, C.I. Garcia, A. DeArdo, New rail steels for the 21st century, Railway Track and Structures 104 (2008) 17–21.
[13] R. Ordonez Olivares, C.I. Garcia, A.J. DeArdo, S. Kalay, Development of high performance steels for rail applications, in: Proceedings of the 2010 Joint Rail Conference High-Speed and Intercity Passenger Rail, April 27–29, 2010 (JRC2010-36082).
[14] F.C. Robles Hernández, R. Ordóñez Olivares, D. Szablewski, C.I. Garcia, A. DeArdo, S. Kalay, Development of the next generation rail steels for heavy axle loads, in: Proceedings of the International Heavy Haul Conference, Shanghai, China, June 22, 2009.
[15] ASTM E45 - 05e2 Standard Test Methods for Determining the Inclusion Content of Steel.
[16] ASTM E1245 - 03(2008) Standard Practice for Determining the Inclusion or Second-Phase Constituent Content of Metals by Automatic Image Analysis.
[17] J. Reiter, C. Bernhard, H. Presslinger, Austenite grain size in the continuous casting process: metallographic methods and evaluation, Mater. Charact. 59 (2008) 737–746.
[18] M.G.M. Fonseca Gomes, L. Henrique de Almeida, L.C.F.C. Gomes, I.L. May, Effects of microstructural parameters on the mechanical properties of eutectoid rail steels, Mater. Charact. 39 (1997) 1–14.
[19] G.K. Bouse, I.M. Bernstein, D.H. Stone, Role of alloying and microstructure on the strength and toughness of experimental, rail steels, in: Symposium on Rail Steels, ASTM, Denver, Colorado, 1976.
[20] E.M. Taleff, C.K. Syn, Pearlite in ultrahigh carbon steels: heat treatment and mechanical properties, Met. Mater. Trans. A 17 (1995) 111–118.
[21] T. Gladman, I.D. McIvor, F.B. Pickering, Some aspects of the structure–property relationships in high-carbon ferrite-pearlite steels, JISI 210 (1972) 916–930.
[22] E.O. Hall, The deformation and ageing of mild steel: III Discussion of Results, Proc. Phys. Soc. Lond. Sect. B 64 (1951) 747.
[23] F. Louchet, J. Weiss, T. Richeton, Hall–Petch law revisited in terms of collective dislocation dynamics, Phys. Rev. Lett. 97 (2006) 075504.
[24] A. DeArdo, R. Ordoñez, C.I. Garcia, S. Kalay, D. Szablewski, F.C. Robles Hernandez, Railroad Steels Resistant to Rolling Contact Fatigue, Patent Application S/N. 12/698,344, February, 2010 Submitted to the U.S. Patent and Trademark Office by J. C. Sloan.
[25] G. Krauss, Steels: Heat Treatment and Processing Principle, ASM International, 2000.